S

APR 27 1998 Sta. 37 (20)

ENGINEERING DATA TRANSMITTAL

1. EDT 620804

2. To: (Receiving Organization) Distribution	3. From: (Originating Organization) SNF Characterization Project/2T720	4. Related EDT No.: N/A
5. Proj./Prog./Dept./Div.: SNFP	6. Design Authority/ Design Agent/Cog. Engr.: L. A. Lawrence	7. Purchase Order No.: N/A
8. Originator Remarks: For Approval and Information		9. Equip./Component No.: N/A
		10. System/Bldg./Facility:
11. Receiver Remarks: 11A. Design Baseline Document? [] Yes [X] No		12. Major Assm. Dwg. No.: N/A
		13. Permit/Permit Application No.: N/A
		14. Required Response Date:

15. DATA TRANSMITTED

(A) Item No.	(B) Document/Drawing No.	(C) Sheet No.	(D) Rev. No.	(E) Title or Description of Data Transmitted	(F) Approval Designator	(G) Reason for Transmittal	(H) Originator Disposition	(I) Receiver Disposition
1	HNF-2191, Rev. 0		0	RELEASE OF WATER TRAPPED IN DAMAGED FUEL SUBSURFACE VOIDS	N/A	1,3	1	

16. KEY

Approval Designator (F)	Reason for Transmittal (G)	Disposition (H) & (I)
E, S, Q, D or N/A (see WHC-CM-3-5, Sec.12.7)	1. Approval 4. Review 2. Release 5. Post-Review 3. Information 6. Dist. (Receipt Acknow. Required)	1. Approved 4. Reviewed no/comment 2. Approved w/comment 5. Reviewed w/comment 3. Disapproved w/comment 6. Receipt acknowledged

17. SIGNATURE/DISTRIBUTION
(See Approval Designator for required signatures)

(G) Reason	(H) Disp.	(J) Name (K) Signature (L) Date (M) MSIN	(G) Reason	(H) Disp.	(J) Name (K) Signature (L) Date (M) MSIN
		Design Authority	1	/	A.L. Pajunen 4/22/98
		Design Agent 3/27/98			
1	/	Cog.Eng. L.A. Lawrence H0-40			
1	/	Cog. Mgr. R.P. Omberg 4/23/98 H0-40			
		QA			
		Safety			
		Env.			

18.	19.	20.	21. DOE APPROVAL (if required) Ctrl. No.
F. F. Huang 3/27/98 Signature of EDT Originator Date	Authorized Representative for Receiving Organization Date	R. O. Omberg 4/23/98 Design Authority/ Cognizant Manager Date	[] Approved [] Approved w/comments [] Disapproved w/comments

RELEASE OF WATER TRAPPED IN DAMAGED FUEL SUBSURFACE VOIDS

F. F. Huang
Fluor Daniel Northwest, Inc., Richland, WA 99352
U.S. Department of Energy Contract DE-AC06-96RL13200

EDT/ECN: 620804 UC: 2070
Org Code: 2T720 Charge Code: LB026
B&R Code: EW7040000 Total Pages: ~~59~~ 61

Key Words: Canister pressurization, K Basin, sludge, water, hydrate

Abstract: Flow rate calculations were undertaken to examine the problem of the release of water trapped in subsurface voids during the vacuum drying for damaged fuel. To calculate the flow rates of the water vapor, five flow models are developed based on the kinetic theory of gases. The difference between the vapor pressure and the operating pressure provides the driving force for crevice water removal. Gas flow is divided into three types: viscous flow, molecular flow, and slip flow in the transition range. These calculations were focused on assessing that measured moisture release from the whole element drying studies currently in progress includes any water that may be trapped in subsurface voids.

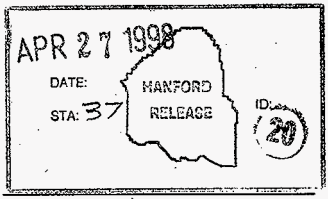

Release Approval Date

Release Stamp

Approved for Public Release

RELEASE OF WATER TRAPPED IN DAMAGED FUEL SUBSURFACE VOIDS

F. F. Huang
Fluor Daniel Northwest, Inc.
Richland, Washington

March 1998

Prepared for
Duke Engineering & Services Hanford, Inc.
Richland, Washington

EXECUTIVE SUMMARY

Uranium metal reacts actively with water to produce uranium oxide and hydrogen gas, and radiolysis of water also produces hydrogen in fuel containers. These fuel reactivities increase the potential for over-pressurization and pyrophoric events during storage. For these reasons, the water content in spent nuclear fuel will be reduced by heat and vacuum. In the conditioning process, free water is expected to be removed by vacuum drying at 50 ° to 75 °C, while chemically bound water can be released during storage at temperatures calculated to be as high as 150 °C.

The following calculations were undertaken to examine the problem of the release of water trapped in subsurface voids during the vacuum drying cycles. Measured moisture release is being studied by performing the whole element drying testing currently in progress; these calculations were focused on assessing that release of moisture includes any water trapped in subsurface voids. These calculations also add insight into the moisture release mechanism during the post Cold Vacuum Drying (CVD) pressure rise test for product acceptance.

Free water will boil as the pressure in the vacuum system decreases, it then cools rapidly and is removed from the system. However, water trapped in damaged fuel subsurface voids has to evaporate and then flow out through cracks and small openings to the surface. Water filling the pores or cracks in fuel will evaporate from the open end; the water interface will recede inward at a rather high rate. To calculate the flow rates of the vapor, five flow models are developed based on the kinetic theory of gases. The long tube

model assumes that water is contained in a pocket of a diameter much larger than the diameter of the long tube that connects the pocket to the surface. The orifice model is similar to the long tube model except for the very short tube. The filled pore model has water in the tube without a pocket. The porous bed flow model has water and a bed of granular particles filled in the tube without a pocket. Calculations show that water can evaporate easily in the pocket. The difference between the vapor pressure and the operating pressure provides the driving force for crevice water removal. Analysis of gas flow considers the flow behavior from comparisons of the molecular mean free path and a tube dimension, from which gas flow is divided into three types: viscous flow, molecular flow, and slip flow in the transition range.

The flow rates of the five models are calculated for each of the three flow types. The rate of orifice flow is much higher than that of long tube flow, and water filled in pores of length 5 cm can be cleared in minutes during the CVD process. Because most of the defects in N Reactor fuel have a radius ranging from 10 μm to 100 μm, and the drying temperature is around 50 °C, the flow of water vapor through defects is slip flow in the transition range. Results show that the long tube flow rate of water vapor decreases significantly with defect radius below 100 μm and that the pocket and defect sizes may be estimated by performing whole element tests. The method to determine the values of pocket and defect sizes by performing pressure rise tests on damaged fuel elements is discussed.

CONTENTS

LIST OF FIGURES

LIST OF TABLES

LIST OF TERMS

a	Defect radius
A	Cross section of defect tube
D	Pocket diameter
d	Defect diameter
δ	Molecular diameter
η	Viscosity of gas
F_t	Flow conductance of tube void
F_o	Flow conductance of orifice void
F_v	Viscous conductance
G	Rate of vapor mass
H	Defect perimeter
K	Constant in orifice flow conductance
κ	Boltzmann constant
ℓ	Length of defect tube
L_a	Mean free path
M	Molecular mass in gram
M_w	Residual water mass
m	Mass of vapor
N	Number of vapor molecule
N_A	Avogadro number
n	Number of mole
P	Pressure
P_g	Average pressure
Q	Flow rate
R	Gas constant
ρ	Density
T	Temperature in K
t	Time
v	Number of vapor molecule striking unit area per unit time
v_a	Mean velocity of molecule
v_{rms}	Root-mean-square molecule velocity
w	Mass flow rate
w_t	Measured mass flow rate
y	Distance of water-vapor interface from the opening
Z	A constant in terms of a and P in a mass flow rate equation

This page intentionally left blank.

RELEASE OF WATER TRAPPED IN DAMAGED FUEL SUBSURFACE VOIDS

1.0 INTRODUCTION

The purpose of removing uranium fuel from the K Basin wet storage to the 200 Area dry storage is to achieve a non-corrosive and stable condition for storing the fuel over an extended period of time. Water in damaged fuel will be subjected to chemical reactions and radiolysis, causing over-pressure and corrosion problems in storage containers. Free water and chemically bound water can be removed by applying heat and vacuum. Sufficient energy will be provided to remove adsorbed and free water during the process of Cold Vacuum Drying (CVD). Hydrates are expected to decompose during staging at moderate temperatures.

Wet fuel will be vacuum dried to remove free water. The amount of water remaining in the element following CVD is therefore of concern for long term storage. Tests on single fuel element under the CVD and staging conditions are in progress to measure the water content after CVD (Ritter 1997; Marschman 1998). Calculations are performed based on existing theories to predict the pressure increase resulting from release of water by heat and vacuum. The pressure profile in single element canisters during staging following the CVD has been studied in a separate report (Huang 1997). In this report, the flow behavior of water vapor trapped in subsurface voids through various defect shapes is investigated.

During the CVD process the dryness of spent nuclear fuel will be evaluated by a moisture monitor. As the pressure in the vacuum system decreases to the partial pressure of water at the container temperature, the free water begins to boil and cools rapidly. It is then removed until equilibrium pressure and temperature in the vacuum system are reached. While the free water on the fuel surface boils and is removed, the water trapped in subsurface voids in the fuel will take a longer time to escape. The flow rate from the subsurface voids varies significantly depending on the size of defect. Some of the water may take a long time to flow out from subsurface voids so that the moisture monitor may not be capable of detecting whether the trapped water has been removed in a short test duration. Therefore, the transport behavior of trapped water is analyzed to determine if it presents problems for the CVD of fuel.

Measured moisture release is being studied by performing the whole element drying testing currently in progress (Marschman 1998); these calculations were focused on assessing that release of moisture includes any water trapped in subsurface voids. These calculations also add insight into the moisture release mechanism during the post CVD pressure rise test for product acceptance.

This page intentionally left blank.

2.0 WATER EVAPORATION

Water tends to evaporate when exposed to a gaseous atmosphere; the rate of evaporation is dependent on its molecule energy, mainly its temperature. At 50 °C, some of the water molecules have sufficient energy to break away from the water surface and enter the air in the vapor state. Eventually some of the water molecules will re-enter the water surface when an equilibrium condition is reach in which the rate of evaporation is equal to the rate of condensation. In this condition, the air above the water is saturated with water vapor molecules, and the pressure on the water surface is called the vapor pressure. The rate of the vapor mass striking the surface is given by (see Appendix A for derivation of the equation).

$$G = P\sqrt{(M/2\pi RT)} \tag{1}$$

At 50 °C, the vapor pressure given in the Steam Table (ASME 1983) is

$$P = 1.7891 \text{ psi} = 0.1217 \text{ atm}$$

$$R = 0.08206 \text{ atm-l/mol-K} \tag{2}$$

$$M = 18 \text{ g/mole}; \; T = 323 \text{ K}$$

$$G = 1.265 \text{ g/cm}^2 \text{ per second}$$

The rate of evaporation shown in Equation (1) predicts that the water in a void of 1 cm^3 will evaporate in about 1 second from a free surface at 50 °C. The water molecules are released from the surface quite rapidly if the pressure of the surrounding air is lower than the vapor pressure of water.

This page intentionally left blank.

3.0 FLOW OF TRAPPED VAPOR

Although water evaporates rapidly under vacuum it may take some time for the water vapor to flow through a long tube with a small diameter before it is removed out of the vacuum system. One important parameter for gases in a vacuum system is the mean free path, which is the average distance traveled before collision with another molecule. The flow rate of gas depends on how large the mean free path of a molecule as compared to the characteristic dimension of the tube through which the gas is flowing. Because the higher the pressure the smaller the mean free path, collisions between molecules are more frequent than those between molecules and the tube wall under high pressures; the flow of an individual molecule is determined by the neighboring molecules and their net motion. In the high-pressure condition of vacuum system, the gas is considered to be viscous, the flow is analyzed hydrodynamically and is called viscous flow. The flow at high pressures can be either laminar or turbulent which generally occurs at very high gas velocities.

On the other hand, at low pressures the flow is called molecular flow because the mean free path is large compared to the characteristic dimension and the flow is predominated by molecular collisions with the walls of the tube; thus, molecular flow is dependent on the geometry of the tube and density differentials. When both types of collisions are important the flow is in the transition range. Therefore, the flow rates are formulated based on the ratio of mean free path (L_a) and characteristic dimension (a) (Knudsen number) as follows.

$$\text{Viscous Flow: } L_a/a < 0.01$$

$$\text{Molecular Flow: } L_a/a > 1.00 \qquad (3)$$

$$\text{Slip Flow in Transition Range: } 0.01 < L_a/a < 1.00$$

A flow rate is defined as the product of volumetric flow rate and pressure as follows:

$$Q = P\, dV/dt = \kappa T\, dN/dt \qquad (4)$$

using the ideal gas law. T in Equation (4) is in K, κ is Boltzmann constant, and dN/dt is the number of molecules per unit time; the Q is directly proportional to a molecule current. The flow rate is sometimes written as the product of pressure difference and conductance which is

$$F = Q/(P_2 - P_1)$$

Since the mass of one molecule of water vapor is 2.99×10^{-23} g, the mass flow rate, w, is calculated from the following equation:

$$\begin{aligned} w &= 2.99 \times 10^{-23}\, Q/\kappa T = MQ/RT \\ &= 2.1656 \times 10^{-6}\, F(P_2 - P_1)/T \text{ g/s} \end{aligned} \qquad (5)$$

where Q is in $Pa \cdot cm^3 \cdot s^{-1}$ and T is in K. In estimating the mass flow rate of water vapor, the flow type is first determined by checking the criteria established in Knudsen number (3) with defect size and average pressure, the flow conductance (F) for the flow type determined is then computed using the flow rates for viscous, molecular, and slip flow to be presented in the following sections. With P and T known under the operating conditions the mass flow rate can be evaluated from Equation (5).

3.1 MEAN FREE PATH

The mean free path (L_a) is defined as the average distance traveled by a molecule. For an equilibrium simple gas of hard sphere molecules the value of L_a is related to the molecular diameter of δ by (Bird 1976)

$$L_a = \frac{1}{\sqrt{2}\pi N \delta^2}$$
$$\delta = \left(\frac{5}{16\eta}\right)^{1/2} \left(\kappa \frac{mT}{\pi}\right)^{1/4} \qquad (6)$$

where n is the number of molecules per cubic centimeter and η is the viscosity of the gas.

As shown in Equation (6), both mean free path and viscosity are dependent on temperature and pressure. If the average pressure is in micron of Hg the following simple relationship between mean free path and pressure is widely used for approximation (Weissler 1979)

$$L_a \approx 5/P_g \qquad P_g \text{ in micron of Hg}$$
or
$$a/L_a \approx 2aP_g \qquad P_g \text{ in Pa} \qquad (7)$$

where $P_g = (P_2 + P_1)/2$. Substituting the mean free path into the division given in the criteria in (3) leads to

$$\text{Viscous Flow: } aP_g > 50$$
$$\text{Molecular Flow: } aP_g < 0.5 \qquad (8)$$
$$\text{Slip Flow in Transition Range: } 0.5 < aP_g < 50$$

For example, the flow of gas in a long hole with a diameter of 0.1 cm under an average pressure of 800 Pa (6 Torr) in vacuum system is viscous flow when aP_g = 0.1 (cm) x 800 (Pa) = 80 > 50.

3.2 VISCOUS FLOW

The rate of flow through a straight tube of circular cross section is calculated using the Poiseuille equation:

$$Q = \frac{\pi a^4}{8\eta\ell} P_g (P_2 - P_1) \quad (9)$$

where:

a = Tube radius

ℓ = Tube length

η = Viscosity of gas

The equation is applicable with assumptions that the gas is incompressible, the flow-velocity is constant and zero at the tube walls, and there is no turbulent motion of gas.

The time required for water vapor to flow from a pocket inside a damaged fuel element to the low pressure area can be estimated by using Equation (9). Figure 1a depicts a void of $\pi D^3/6$ with a long hole leading to the surface of fuel element. The pocket is half full of one gram of water. As estimated in Section 2, it takes only 1 second to evaporate one gram of water at 50 °C. The steam pressure is given in ASME Steam Table (ASME 1983):

a = 0.1 cm; ℓ = 5 cm; T = 323 K; P_2 = 1.7891 psi = 12334 Pa

P_1 = 3 Torr = 400 Pa; P_g = 47.76 Torr = 6367 Pa

$\eta = 10.6 \times 10^{-6}$ Pa s; $\kappa = 1.38 \times 10^{-23}$ J/K

The flow is viscous flow as $aP_g = 636 > 50$ (see Criteria 8). Thus, from Equation (9) we have $Q = 2.63 \times 10^5$ Pa·cm^3·s^{-1}. Using Equation (5) the number of molecules that cross the plane per unit time can be estimated. The mass of water crossing the plane per second (w) is equal 3.52×10^{-3} g. Therefore, it takes about 5 minutes for the water vapor of 1 g to flow from the pocket to the opening of the long tube with a radius of 0.1 cm.

If water fills up the 5-cm channel the water in the pocket may not evaporate before the channel is cleared. In this case the water at the end of channel subjected to the low pressure will evaporate first with a rate of $1.265 \times \pi$ (0.1 x 0.1) = 0.04 g/s. However, as the water interface in the tube recedes, it will take a longer time for the water vapor to flow out of the tube. This subject will be discussed in more detail in Section 4.2.

3.3 MOLECULAR FLOW

For conditions of $aP_g < 0.5$ where the mean free path is greater than the characteristic dimension, the molecular flow rates for flow through long tubes and orifices are given below (Knudsen 1911).

Flow Through Long Tubes

The conductance of a long tube of length ℓ, variable cross section A, and perimeter H calculated by Knudsen is

$$Q = \frac{4}{3} \frac{v_a}{\int \frac{H}{A^2} d\ell} (P_2 - P_1) \tag{10}$$

where v_a is given in Equation (A6). For a cylindrical tube of radius a and length of ℓ, the flow rate is

$$\begin{aligned} Q &= F_t(P_2 - P_1) \\ F_t &= 2\pi/3(a^3/\ell)v_a = \sqrt{(32\pi/9)}(a^3/\ell)(RT/M)^{1/2} \ s^{-1} \end{aligned} \tag{11}$$

where

$$R = 8.3133 \times 10^6 \ Pa \cdot cm^3 \cdot deg^{-1} K \cdot g\text{-}mole^{-1}$$

Flow Through Orifices or Short Tubes (Dushman 1922)

$$\begin{aligned} Q &= F_o(P_2 - P_1) \\ F_o &= \tfrac{1}{4}K(\pi a^2)v_a = \sqrt{(\pi/2)}Ka^2(RT/M)^{1/2} \ s^{-1} \end{aligned} \tag{12}$$

where:

$$K = (1 + 3\ell/8a)^{-1}$$

and

$$R = 8.3133 \times 10^6 \ Pa \cdot cm^3 \cdot deg^{-1} K \cdot g\text{-}mole^{-1}$$

As:

$F_o/F_t = 3\ell/8a$, $F_o = F_t$ when $\ell/a = 8/3$.

3.4 SLIP FLOW IN TRANSITION RANGE

As the pressure decreases to a pressure below the viscous limit, the flow velocity at the tube walls becomes significant and contributes an additional conductance as "slip" correction. In this transition range, both viscous flow and molecular flow are influential in evaluating the rate of slip flow. With an operating pressure of 400 Pa and the water vapor pressure of 12300 Pa at 50 °C, slip flow is important if the radius of pore is in the range of 10 μm to 100 μm, according to the criteria in (8) ($0.5<aP_g<50$). As shown in Figure 2, the crack size in fuel elements is about 30 μm; the flow rate of water vapor in defects can be estimated more accurately by considering viscous flow corrected for slip.

The flow rate for slip flow in the transition range is given by (see Appendix B for details)

$$F = F_t(F_v/F_t + Z)$$

$$= F_t(0.1472(a/L_a) + Z) \qquad (13)$$

$$Z = (1 + 2.507(a/L_a))/(1 + 3.095(a/L_a))$$

Equation (13) also can be written in terms of viscous conductance F_v:

$$F = F_v\ (1 + 7.793(L_a/a)Z) \qquad (14)$$

The mean free path L_a is dependent on the average pressure P_g. At high pressures, a/L_a is large, and Z approaches a small value of 0.81 compared to the value of F_v/F_t in Equation (13), thus, the flow is predominated by viscous flow. On the other hand, when a/L_a is small at low pressures, Z approaches 1 and F_v/F_t becomes small, the conductance F approaches molecular flow F_t. Figure 3 shows a semi-log plot of F/F_t as a function of a/L_a to illustrate the type of flow. The value of mean free path of saturated steam given previously is used to evaluate its ratio to defect radius: $a/L_a = 2\ aP_g\ (cm \cdot Pa)^{-1}$. This ratio is used to calculate the rate of slip flow from Equations (13) or (14).

This page intentionally left blank.

4.0 CALCULATION

Water trapped in a pocket with a short tube and large orifice can evaporate easily at 50 °C under vacuum as shown in Equation (2). For water pockets with a long and small cross section tube, water may partially fill the pockets or alternately they may be filled up to the end of the tube. In some fuel defects water may fill the pores without subsurface pockets as shown in Figure 1b. The water-air interface may be anywhere in the pocket or the tube. From the free surface of the interface water molecules will break away as discussed in Section 2.0 and provide pressure difference as a driving force for water removal. To estimate the flow rate of water vapor through defects, flow models are developed with assumptions that all voids have a pocket and a long tube or orifice, or they have only pores filled with water. The flow rates for water interface in a pocket or a pore are estimated based on the flow rate equations given above.

4.1 LONG TUBE MODEL

The long tube model is depicted in Figure 1a for a fuel crevice. Water is deposited in the pocket ready for evaporation at temperatures maintained at 40 °C or higher during the CVD. The long tube leading to the surface of fuel is empty for vapor to flow toward low pressure space. As an example, the flow rate of water vapor at 50 °C through a tube with a length of 5 cm and a diameter of 100 μm is computed as follows. The test conditions are the same as those listed in Section 3.2. Firstly, the criteria in Equation (8) are checked to determine the type of flow. With a = 50 μm = 50 x 10^{-4} cm, P_g = 6367 Pa, and $0.5 < aP_g = 32 < 50$, the flow is found to be slip flow in transition range according to the criteria in (8). Using Equations (11) and (13) we found that $F_t = 1.020 \times 10^{-3}$ cm^3/s and $F = 9.545 \times 10^{-3}$ cm^3/s. For long tube flow, the mass flow rate in terms of a is estimated from the same equations to be:

$$w_1 = 0.00492 \times (P_2 - P_1) \times (0.1472a(P_2 + P_1) + Z)a^3/(\ell T^{1/2}) \text{ g/s}$$
$$Z = (1 + 2.507a(P_2 + P_1))/(1 + 3.095a(P_2 + P_1)) \qquad (15)$$

where a and ℓ are in cm, P is in Pa, and T is in K. The value of a/L_a is estimated from Equation (7) to be 63.67, the following results are obtained:

$aP_g = 32 < 50$ (slip flow)

$Z = 0.811$; $F_v/F_t = 9.387$

$w_1 = 8.319 \times 10^{-7}$ g/s

$= 2.995 \times 10^{-3}$ g/h

The mass flow rate is computed from flow conductance with Equation (5). Figure 4 shows the mass flow rate in terms of defect radius up to 500 μm for temperatures of 40 °C, 50 °C, and 75 °C. The time, $t = m/w_1 = \pi\rho D^3/6w_1$,

required to remove the water in a pocket of 1 cm diameter (about 0.53 g) through a 5-cm long tube with a radius of 50 μm is about 180 hours. For tubes of much smaller cross sections, as the one shown in Figure 2 where the diameter of a crack is about 30 μm, it may take months for the water to flow out of the channel. As shown in Figure 5, the time required for water vapor to flow out from a long tube increases rapidly with tube radius smaller than 100 μm.

4.2 FILLED PORE MODEL

If water is filled in a pore with interface close to the opening of the channel, water vapor will flow through the orifice, and the water interface is lowered until y = 8a/3 when orifice flow conductance (F_o) is equal to molecular flow conductance (F_t) (Figure 1b); below that height the flow conductance is calculated using the rate equation of the long tube model. Upon evaporation the interface recedes with time as expressed by (see Appendix C):

$$y = (20.68at - 0.0053)^{1/2}$$
$$t = (y^2 + 0.0053)/20.68a \qquad \text{(C3)}$$

At y = 5 cm and a = 50 μm, t = 241.8 s. Neglecting the small value of y for orifice flow, the mass flow rate of a filled pore, which is time dependent, is given by

$$w_2 = 0.00492x(P_2-P_1)x(0.1472a(P_2+P_1)+Z)a^3/((20.68at - 0.0053)T)^{1/2} \text{ g/s}$$
$$Z = (1 + 2.507a(P_2 + P_1))/(1 + 3.095a(P_2 + P_1)) \qquad (16)$$

for

$$0.053 \leq t \leq (\ell^2 + 0.0053)/20.68a$$

The mass flow rate decreases with increasing time or the distance between the opening and the interface. The rate continuously declines until the interface reaches the end of the pore where the mass flow rate equals the rate for the long tube model with the same tube length (Figure 6). Because of higher flow rates it does not take long to remove the water in the filled tube (241.8 seconds for a defect of the size given above).

4.3 ORIFICE MODEL

A water pocket may be located beneath a cladding defect (Figure 1c). The mass flow through an orifice is computed by Equations (12) and (13). For cladding with a thickness of 0.07 cm, the mass flow rate is given by

$$w_o = 1.845x10^{-3}x(1 + 0.02625/a)^{-1}(0.1472a(P_2+P_1) + Z)(P_2-P_1)a^2T^{-½} \text{ g/s}$$
$$Z = (1 + 2.507a(P_2 + P_1))/(1 + 3.095a(P_2 + P_1)) \qquad (17)$$

The mass flow rate for orifice model as a function of defect size is plotted in Figure 7. With residual water of 1 g, the time to remove the free water through orifice is shown in Figure 8. A comparison between Figures 4 and 7 indicates that the orifice flow rate is 60 times higher than that from the long tube model. At 50 °C and a = 50 μm, the mass flow rate of the orifice model is found to be $w_o = 4.86 \times 10^{-5}$ g/s, which is lower than the flow rate (1.3×10^{-4} g/s) under the same conditions computed from an orifice model proposed by Pajunen. However, the rate of the former orifice model increases faster than that of the latter as the defect size increases into the viscous flow range as seen in Figure 9.

4.4 EXHAUST OF WATER VAPOR

The flow rates evaluated above are based on the constant vapor pressure maintained by the water in a pocket at the operating temperature. The water continues to evaporate as the vapor flows out through a tube or orifice. In the case where only water vapor is present, the pressure in the void of volume V changes with time and the conductance F varies with pressure, the rate of exhaust is given by $-VdP/dt = FP$. Let P_o designate the pressure in the vacuum system during the exhaust. Using Equations (7) and (13), we obtain

$$-Vd(P - P_o)/dt = F_t(0.1472a(P + P_o) + Z)(P - P_o) \qquad (18)$$

Solving the differential Equation (18) gives

$$\ln\left(\frac{P_1 - P_o}{P_2 - P_o}\right) - \ln\left(\frac{P_1 - P_o + Z'/0.1472\,a}{P_2 - P_o + Z'/0.1472\,a}\right) = \frac{Z'F_t}{V}(t_2 - t_1) \qquad (19)$$

where P_1 is the pressure at time t_1, P_2 is the pressure at time t_2, and $t_2 > t_1$. For a tube of length 5 cm, radius 50 μm, $F_t = 1.020 \times 10^{-3}$ cm³/s at 50°C and P_o = 400 Pa (3 Torr), and $Z' = Z + 0.2944aP_o$, the following results are obtained:

P_1 = 12334 Pa (92.53 Torr), P_2 = 1593.3 Pa, $t_2 - t_1 = 799.5V$ sec/cm³;

P_1 = 1593.3 Pa (11.95 Torr), P_2 = 519.3 Pa, $t_2 - t_1 = 1438.3V$ sec/cm³;

P_1 = 519.3 Pa (3.90 Torr), P_2 = 411.9 Pa, $t_2 - t_1 = 1591.0V$ sec/cm³.

It takes a total of 64 minutes to exhaust the vapor from a 1-cm³ pocket through a long tube to an vacuum environment of 400 Pa at 50 °C. Results also show that the time required to reduce the pressure 10% increases with decreasing pressure. Compared to the long tube flow rate (w_1), the rate of vapor exhaust is about 35 times slower because the flow conductance decreases with time at the stated pressure.

4.5 POROUS BED FLOW MODEL

The defects shown in Figure 2 suggest that the fuel is likely to have pores or cracks packed with a bed of dense swarm of particles. The driving force from steam pressure for flow to the fuel element surface is similar to that for the filled pore model described in Section 4.2. Considering the bed of granular particles as a porous mass, the flow rate of water vapor through a porous mass is calculated using an empirical relation of Darcy's equation:

$$v = -(k/\eta)\text{grad } P \tag{20}$$

where:

v = The rate of flow through a surface element of unit area

k = The permeability of the porous mass

P = The pressure

Equation (20) is modified to maintain the equilibrium between the forces acting on a volume element of fluid - the pressure gradient, the divergence of the viscous stress tensor and the damping force caused by the porous mass (Brinkman 1947). The modified equation is in the form of

$$\text{grad } P = -(\eta/k)v + \eta'\Delta v \tag{21}$$

This equation is good for a wide range of permeability of the porous mass. For low values of k, Equation (21) is approximated to be Equation (20); if k is large, the first term on the right hand side of Equation (21) is neglected. A solution can be obtained by imposing Equation (21) with the condition of incompressibility: div v = 0. Let the total volume of N particles of radius R and the volume of pore be V_o and V, respectively,

$$V_o = (4\pi/3)R^3N,\ V = \ell\pi a^2$$

Assuming $\eta' = \eta$, the rate of flow is

$$v = \frac{\pi D_p^2 a^2}{18\eta V_o}\left[1 + \frac{3V_o}{4V}\,1 - \sqrt{\left(\frac{8V}{V_o} - 3\right)}\right](P_2 - P_1) \tag{22}$$

Using the bed voidage and the diameter of particle given in (Pajunen 1997), the N, D_p, V_o, and V can be estimated as follows:

$\epsilon = 0.6 = 1 - V_o/V$ or $V_o = 0.4\ V$

$D_p = 15\ \mu m = 1.5 \times 10^{-3}$ cm

Substituting these data into Equation (22) gives

$$v = 1.969 \times 10^{-8}\,(P_2 - P_1)/\eta\ell \tag{23}$$

Thus, the mass flow rate of porous bed flow model is given by

$$w_3 = 1.34 \times 10^{-13} a^2 P_g (P_2 - P_1)/(\eta \ell T) \text{ g/s} \quad (24)$$

The mass flow rate of a pore (a radius of 50 μm and a length of 5 cm) with a bed of porous mass at 50 °C can be calculated from Equation (24).

$$w_3 = 1.49 \times 10^{-8} \text{ g/s}$$
$$= 8.94 \times 10^{-7} \text{ g/min}$$

Therefore, the mass flow rate in a 5-cm-long pore with a swarm of particles is about 165 times slower than the one without particles. However, because the rate is dependent on pore length and time, the rate of flow through a dense swarm of particles is much higher when the interface is near the opening of the channel as discussed in Section 4.2 for the filled pore model.

As derived in Appendix C, the length of bed dried in a particular time (t) can be found as follows:

$$y = \frac{D_p}{9} \left\{ \frac{Mt}{\eta (1-\epsilon) RT} \left[1 + \frac{3(1-\epsilon)}{4} \left(1 - \sqrt{\left(\frac{8}{1-\epsilon} - 3 \right)} \right) \right] P_g (P_2 - P_1) \right\}^{1/2} \quad (25)$$

where:

$$P_g = (P_2 + P_1)/2$$

This equation is similar to Equation 9.2-10 in (Pajunen 1997) except that the latter is multiplied by a shape factor. For comparisons the lengths of dried bed are calculated for the two porous bed flow models with the same constants given in Figure 9.2-4 in the Reference. After drying at 50 °C for 1 hour, the lengths of dried bed are calculated to be:

$y = 2.65$ cm from Equation (25), this work

$L_2 = 1.78$ cm from Equation 9.2-10, HNF-1851

The present porous bed model predicts that the cracks filled with porous mass in the damaged fuel is dried faster by 33% than the one proposed in (Pajunen 1997). If the present model considers a shape factor (ϕ_s) of 0.6 for the length of dried bed in the form of

$$L_1 = y \times \phi_s \quad (26)$$

L_1 is found to be 1.59 cm from the present flow model, which is 11% shorter than L_2. Therefore, they appear to agree each other if both are assumed to have a same shape factor.

This page intentionally left blank.

5.0 RESULTS AND DISCUSSION

The mass flow rate of saturated steam flowing through a long or short tube of defects in uranium fuel has been estimated based on the gas flow models. The rate of vapor exhaust is also estimated for fuel defects full of water vapor without liquid. All of the flow rates are found to depend on the water vapor pressure and the size of defect. Without knowledge of the type and size of defect, estimates of residual water inventory and time required to release trapped water from fuel subsurface voids during the CVD are difficult to make. However, rough estimates can be made by assuming the sizes of all fuel defects are the same.

5.1 RELEASE OF TRAPPED WATER

In damaged fuel, water may be trapped in the following one or more types of fuel subsurface voids evaluated (Figure 1):

1. A long tube of radius a and length ℓ constrained by a water pocket of volume V
2. An orifice of radius a with a water pocket of volume V
3. A pore (a and ℓ) without pocket is filled with water
4. A long tube and a pocket like Type 1 defect but full of vapor only
5. A pore is filled with water and a bed of granular particles.

For purposes of comparisons, the flow rates and thus the time spent to remove the water vapor from the four types of defect are calculated using the above rate equations with the following assumptions. The ratio of defect length to diameter is 100.

$a = 50\ \mu m$, $\ell = 5$ cm, $V = 1\ cm^3$, m (mass of water) = 0.53 g,

$T = 50\ ^\circ C$, $P = 12334$ Pa, and $P_o = 400$ Pa.

Results are listed in Table 1. Because defect Type 1 contains much more water than Type 4, it takes a longer time to reduce the pressure in Type 1 pocket to the system pressure. The water trapped in other types of defect generally does not take long to flow out of voids during the CVD process.

Defect Types 1 and 2 contain the same amount of water, but the vapor in the latter flows at a much higher rate. The water in defect Type 1 will continue to flow out at a constant rate until no liquid is left, the flow rate then slows down to equal the rate of Type 4. Clearly, the fewer the Type 1 defects in fuel the easier the trapped water will be released. Since the damaged fuel is likely to have more defect Types 2, 3, 4, or 5 most of free water should be removed during the 10-hour CVD process.

Table 1. Mass Flow Rate and Time Required to Release Trapped Water. (a = 50 μm, ℓ = 5 cm, V = 1 cm^3, m = 0.53 g, T = 50 °C)

Defect Type	Mass Flow Rate (g/min)	Time
1. Long tube with liquid in pocket	4.994×10^{-5}	7.5 day
2. Orifice with liquid in pocket	2.92×10^{-3}	3 hour
3. Pore filled with liquid	$6.86 \times 10^{-4} - 4.994 \times 10^{-5}$	4 minute
4. Long tube with only vapor in pocket	6.47×10^{-6}	13 minute
5. Pore filled with liquid and porous mass	$1.21 \times 10^{-5} - 8.94 \times 10^{-7}$	4 hour

5.2 PRESSURE RISE TESTS

The results of similar flow rate evaluations have been used to define pressure rise testing following the cold vacuum drying to demonstrate the residual free water inventory of an Multi-Canister Overpack (MCO) (Pajunen 1997). At a constant temperature of 50 °C and the fuel container maintained at a pressure less than 30 Torr, the pressure increase and test time will be recorded. The measured increase in pressure is obtained by dividing the pressure increase with the test time. This pressure increase is converted to the mass flow rate using the following equation:

$$w_t = MV(P_2 - P_1)/RTt \qquad (27)$$

A measured rate of pressure rise in Torr/hr can be converted to a measured mass rate in g/s through Equation (27). In pressure rise testing, the fuel sample was isolated from flowing gas and vacuum pumping, the pressure increase was monitored and the total water release was measured with a moisture monitor at the CVD conditions. The results of a specimen of undamaged fuel element 1990 is shown in Figure 10 where moisture partial pressure was recorded in terms of time at 53 °C (Marschman 1998). Results show that the moisture partial pressure increases linearly with time during CVD for 1 hour. Because the sample was cut from an undamaged fuel element, there was no water trapped in subsurface voids; the sources of water vapor that contributed the pressure rise was the surface film of the sample.

If the value of measured pressure rise rate (w_t) is higher than that calculated w_1 from Equation (15) or w_o from Equation (17), more than one defect should exist in damaged fuel. The magnitude of w_t is dependent on the type and size of fuel crevice and is equal to the sum of flow rates from all types of crevices present in the sample. The flow mass in defect type 4 is considered to be a small part of defect type 1. To estimate the maximum residual water (M_w) for one type of defect with each defect assumed to be constrained to a spherical water pocket with a diameter of D, the residual water is given by (Pajunen 1997)

$$M_w = w_t \rho (\pi/6) D^3 / w_i \qquad (28)$$

where w_i is w_1, w_2, or w_o given in Equations (15), (16), or (17) which is a function of defect size. As indicated by Equation (28), for a value of w_t selected from pressure rise testing, the residual water can be estimated only if the ratio of water pocket and defect size (diameter ratio D/d) is known because w_i is dependent upon the parameter d. Figures 11 and 12 show the dependence of D/d on w_t and temperature for the long tube model and orifice models for residual water content of 1 gram, respectively. As Figure 11 implies, the ratio D/d is no more than 120 for a pressure rise rate of 3 Torr/h. Converting the pressure rise to w_t using Equation (27) and residual water should be less than 1 gram to meet the selected test criterion. From Figure 4 a single water pocket must be constrained by a defect of radius 50 μm for the selected w_t; thus, the value of D=120 x 100 μ = 1.2 cm confirms 1 g water in the pocket. The result also proves that $w_t = w_1$, and $M_w = \pi D^3/6$, as shown in Equation (28), which indicates that the value of D is obtained only if the amount of residual water is given, and that the value of D/d is unknown unless the entire system has only one single defect and water pocket.

Since the fuel elements contain more than one defect, the relationship between water pocket size (D) and the size (d) of its constrained defect has to be established theoretically or empirically before the residual water in damaged fuel can be estimated.

5.3 ESTIMATE OF RESIDUAL WATER

Assuming the measured increases in pressure are 1×10^{-5} or 1×10^{-4} g/s at 50 °C and 1×10^{-3} g/s at 75 °C for the orifice model, the values of D and a (radius =d/2) can be computed from Equations (15) and (28) for various amount of residual water (Figure 13). Because there are more than one defect, the pocket diameter can be any value other than 1.2 cm for 1 g of residual water depending on the measured increase in pressure (see curves 1, 3, 5 in Figure 13). With the measured pressure rise (w_t) in terms of mass and the known values of D and *a*, the amount of residual water can be estimated from similar plots of D versus *a* constructed for various amounts of residual water. For example, a measured w_t of 1×10^{-5} g/s predicts 1 g of residual water if the values of D/*a* is either 0.75 cm/50 μ (= 75, point x in Figure 13) or 1.17 cm/100 μ (= 58, point y); the residual water content would be 2 g if D is larger (1 cm) with a same value of a (100 μ) as designated by point z in Figure 13. Although the curve of pocket diameter versus defect radius is nearly linear, the ratio D/*a* is not unique in relating to residual water content, as demonstrated by points x and z where both values of ratio D/a are close to 74 but predict different amounts of residual water (1 g and 2 g).

The residual water (M_w) is described by the values of geometric features, D and *a*, for each measured increase in pressure (w_t) at a given temperature (T) as shown in Equation (28). Using Equation (28) the size of defect can be estimated from two pressure rise tests at two different temperatures with two sets of w_t, P, and T. The value of defect radius *a* is calculated from the following equation:

$$f_1(a,P)/f_2(a,P) = (w_{1t}/w_{2t})(P_2^2-P_1)/(P_2^1-P_1)(T_1/T_2)^{1/4} \qquad (29)$$

where:

$$f(a,P) = 0.1472a(P_2+P_1) + (1+2.507a(P_2+P_1))/(1+3.095a(P_2+P_1))$$

With the value of a determined, the mass flow rate can be evaluated and the only unknown variable for estimating the residual water inventory in Equation (28) is pocket diameter D. For pressure rise tests performed at 50 and 75 °C, the defect radius of the damaged fuel element is evaluated as a function of w_{1t}/w_{2t} ratio as shown in Figure 14. The defect size is small for $w_{1t}/w_{2t} < 8$, but becomes sensitive to the rate ratio as it approaches 9.3. The plot shown in Figure 14 indicates that there is a large uncertainty in determining defect size using Equation (28) if the pressure rise rate ratio (75 °C to 50 °C) is larger than 9.3. Since the value of M_w is linearly dependent on D which cannot be evaluated from pressure rise tests, the present analysis is capable of determining the residual water inventory of damaged fuel only if the pocket size of voids can be measured.

On the other hand, the value of D can be calculated from Equation (28) if the amount of residual water is obtained from a whole element test by vacuum and heating at 50 to 75 °C for a long period of time and summing up the total amount of moisture monitored throughout the entire test. Thus, the geometric features of subsurface voids in damaged fuel can be characterized by performing two pressure rise tests at different temperatures and heating the fuel element to a high temperature at the end of the test. The test data will be used to evaluate the pocket and defect sizes for each damaged fuel elements. The following is sample calculation made from results of damaged fuel element 0309M (Oliver 1998).

Results of pressure rise test performed after the CVD at 50 °C are shown in Figure 15. The rate of water vapor pressure increase was 0.28 Torr/hr, the mass flow rate was calculated to be $w_{2t} = 2.25 \times 10^{-4}$ g/s using Equation (27) with V = 10,000 cm^3. There is no pressure rise test performed at other temperatures, $w_{1t} = 1.98 \times 10^{-3}$ g/s at 75 °C is assumed giving $w_{1t}/w_{2t} = 8.8$. Thus, the defect radius and mass flow rate are found to be 40 μm and 1.97×10^{-5} g/s according to Figures 14 and 7, respectively. Because more hydrates will be decomposed to release hydrated water at temperatures higher than 75 °C, only the water released during the entire CVD test is used as the amount of residual water to estimate the pocket size. Results of drying tests on element 0309M show 5 g of water released during the CVD process; therefore, the value of D is calculated to be 0.94 cm. The above data are summarized as follows:

Sample: damaged fuel element 0309M

Test temperature = 50 °C, 75°C

Pressure rise rate $w_{2t} = 2.25 \times 10^{-4}$ g/s at 50°C

Assumed pressure rise rate $w_{1t} = 1.98 \times 10^{-3}$ g/s at 75 °C

Defect mass flow rate w_o = 1.97 x 10^{-5} g/s at 50 °C

Defect radius a = 40 μm

Residual water M_w = 5 g

Pocket diameter D = 0.94 cm

This page intentionally left blank.

6.0 CONCLUSION

Water trapped in fuel subsurface voids will evaporate easily during the cold vacuum drying at 50 °C. The difference between the water vapor pressure and the operating pressure provides the driving force for the vapor to flow out from water pockets. Five flow models are developed to evaluate the flow rates based on the kinetic theory of gases. Depending on defect size the flow rates of long tube and orifice flow models vary significantly; the rates drop rapidly as the defect radius decreases to less than 100 μm. Water trapped in a pore without a pocket evaporates from the open end with the water interface receding at fairly high rates. The flow rate of water vapor through a bed of granular particles is found to be much slower than the rate through a pore filled of only water. In general, most of the water trapped in damaged fuel subsurface voids is expected to be removed in a few hours by cold vacuum drying. The flow behavior of vapor through crevices is analyzed; results of pressure rise tests performed during the CVD process may be used to estimate the initial residual water in the damaged fuel elements provided the geometric features of the voids (D,d) are known.

This page intentionally left blank.

7.0 REFERENCES

ASME 1983, Steam Table, American Society of Mechanical Engineers.

Abrefah, J., et al., 1996, K Basin Spent Nuclear Fuel Characterization Data Report, PNNL-10994, UC-602, Pacific Northwest National Laboratory, Richland, Washington.

Bird, G. A., 1976, Molecular Gas Dynamics, Clarendon Press, Oxford.

Brinkman, H. C., 1947, "A Calculation of the Viscous Force Exerted by a Flowing Fluid on a Dense Swarm of Particles," Applied Science Res., Vol. A1, pp. 27-34.

Dushman, S., 1922, "The Production and Measurement of High Vacua," General Electric Review.

Huang, F. H., 1998, *Pressurization of Whole Element Canister During Staging*, HNF-2047, Rev. 0, Fluor Daniel Northwest, Inc., Richland, Washington.

Kennard, E. H., 1938, "Kinetic Theory of Gases," McGrow-Hill Book Co., New York, New York.

Klinger, G. S., et al., 1998, *Drying Results of K Basin Fuel Element 5744U*, PNNL-11821, UC-602, Pacific Northwest National Laboratory, Richland, Washington.

Knudsen, M., Ann. Physik, 28, 75, 999 (1909); 35, 389(1911).

Marschman, S. C., et al., 1998, *Drying Results of K Basin Fuel Element*, PNNL-11782, UC-602, Pacific Northwest National Laboratory, Richland, Washington.

Oliver, B. M., et al., 1998, *Drying Results of K-Basin Fuel Element 0309M*, PNNL-11820, UC-602, Pacific Northwest National Laboratory, Richland, Washington.

Pajunen, A. L., 1997, *Cold Vacuum Drying Residual Free Water Test Description*, HNF-1851, Rev. 0, SNG Eurisys Services Corp., Richland, Washington.

Ritter, G. A., et al., 1997, *Hanford Spent Nuclear Fuel Cold Vacuum Drying Proof of Concept Test Report*, HNF-SD-SNF-TRP-021, Rev. 0, Fluor Daniel Northwest, Inc., Richland, Washington.

Vincenti, W. G. and C. H. Kruger, Jr., 1975, "Introduction to Physical Gas Dynamics," R. E. Krieger Publishing Company, Huntington, New York.

Weissler, G. L. and R. W. Carson, 1979, "Vacuum Physics and Technology," Academic Press, New York, New York.

This page intentionally left blank.

Figure 1. Flow Models for Water Trapped in Fuel Subsurface Voids (a) Long Tube Model, (b) Filled Pore Model, (c) Orifice Model, (d) Vapor Filled Long Tube Model.

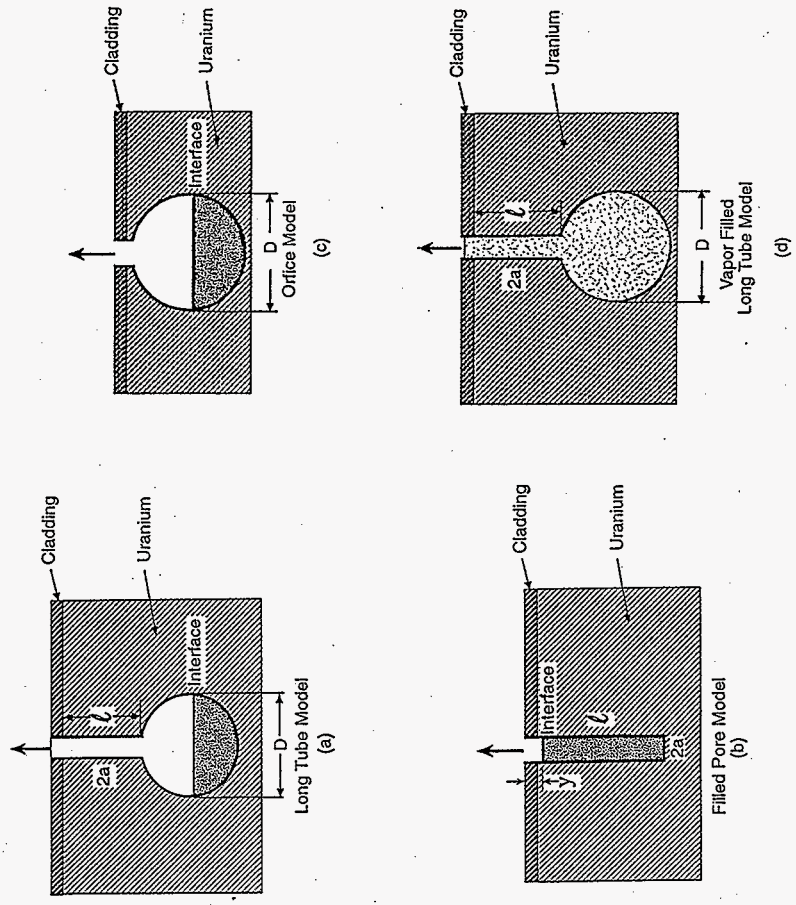

Figure 2. Metallography for Heat Tinted Specimen 5-S1A-A1A Showing Portion of Crack Network, Hydrided Area Along Cracks, and Carbide Inclusions.

SNF-642

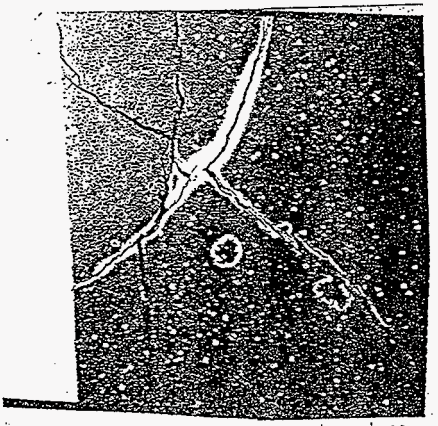

SNF-643

Figure 3. Ratio of Total Conductance to Molecular Flow Conductance (F/F_t) Versus a/L_a for Cylindrical Tube.

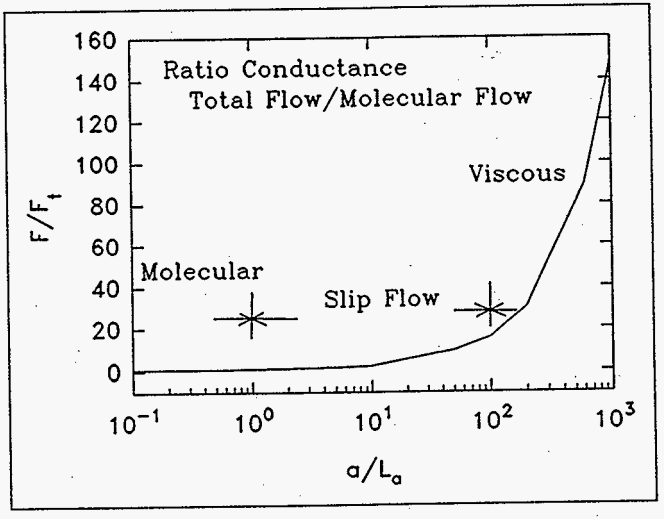

Figure 4. Variation of Mass Flow Rate with Defect Radius for Long Tube Model.

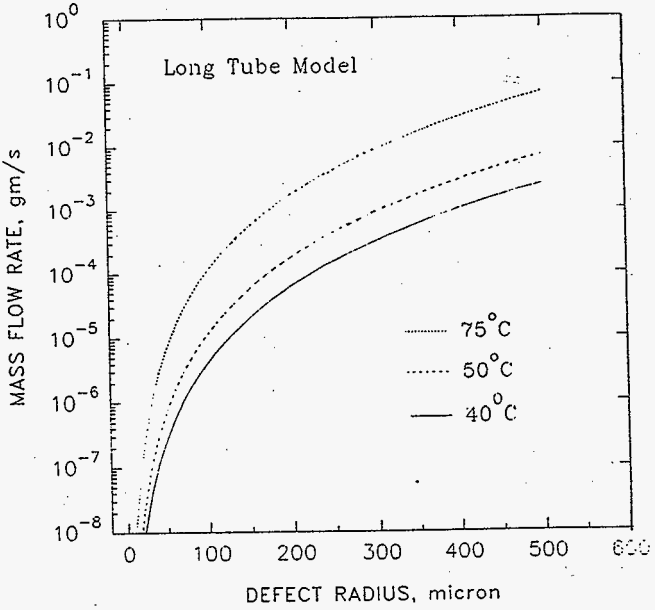

Figure 5. Test Duration Versus Defect Radius for Long Tube Model.

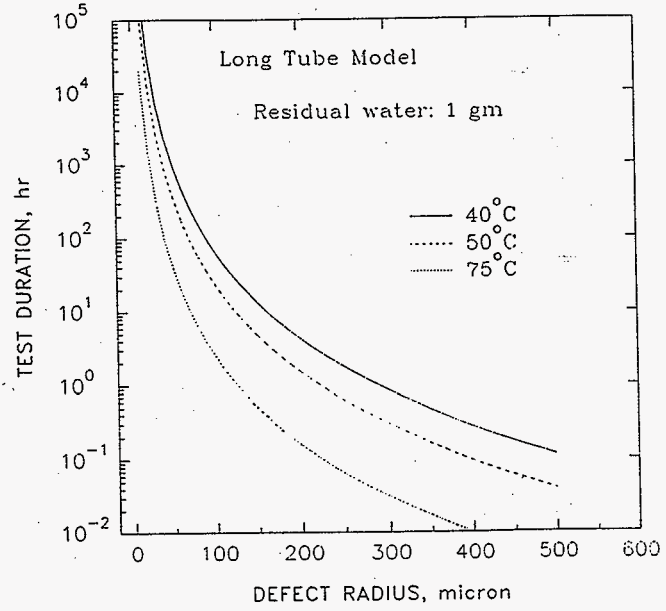

Figure 6. Mass Flow Rate Versus Test Duration for Filled Pore Model.

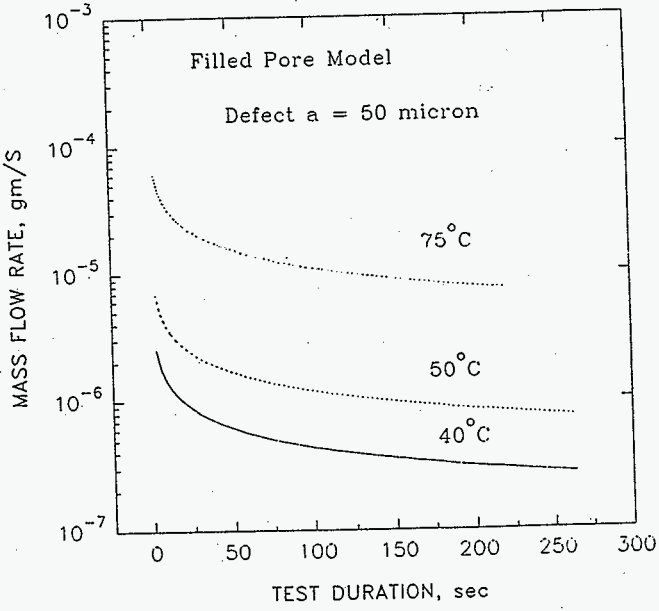

Figure 7. Variation of Mass Flow Rate with Defect Radius for Orifice Flow Model.

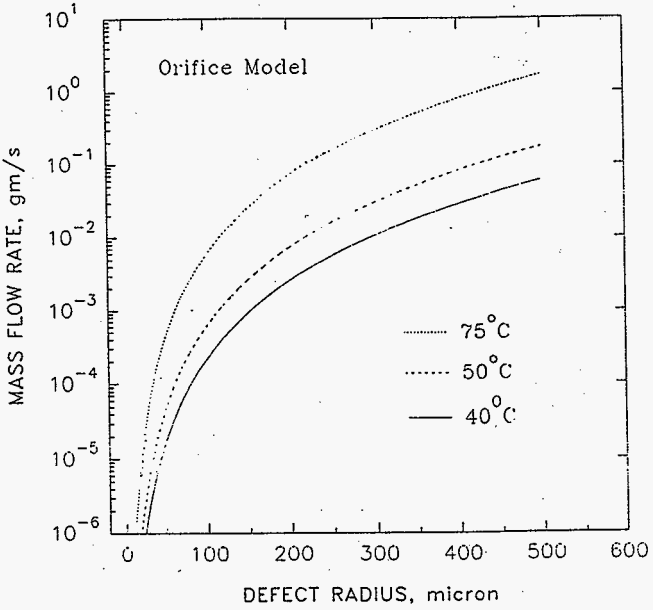

Figure 8. Test Duration Versus Defect Radius for Orifice Flow Model.

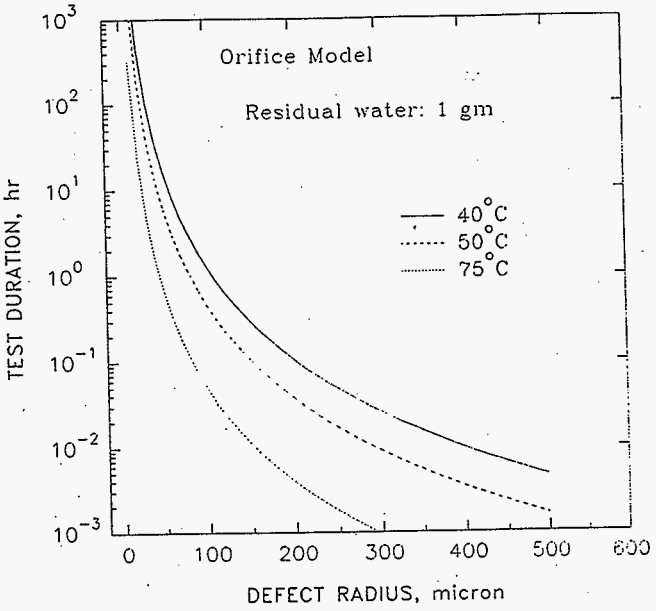

Figure 9. Comparisons of Mass Flow Rates Calculated from Two Different Orifice Flow Models.

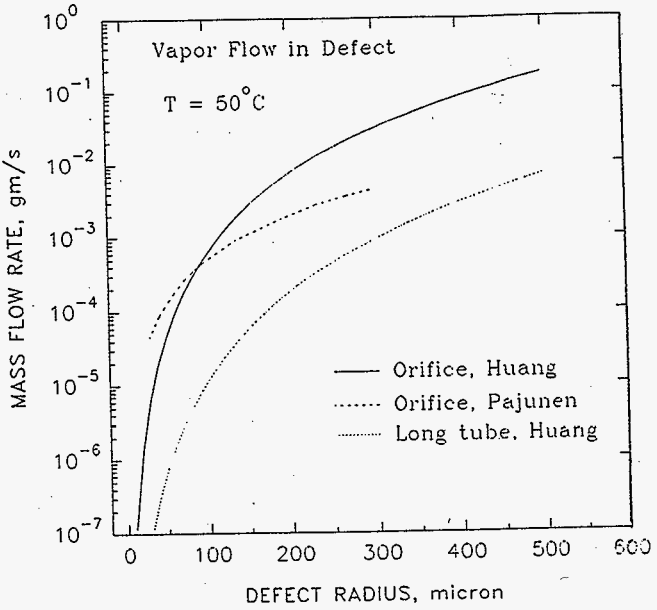

Figure 10. Plots of Pressure Rise Versus Time for Undamaged Spent Nuclear Fuel Element 1990.

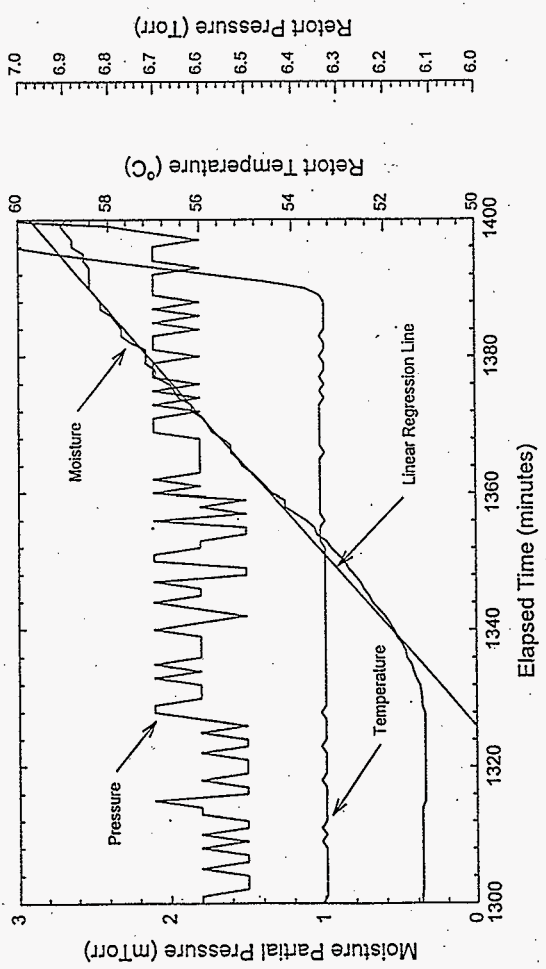

Figure 11. Ratio Pocket Diameter/Defect Diameter Versus Pressure Rise Mass Rate for Long Tube Model.

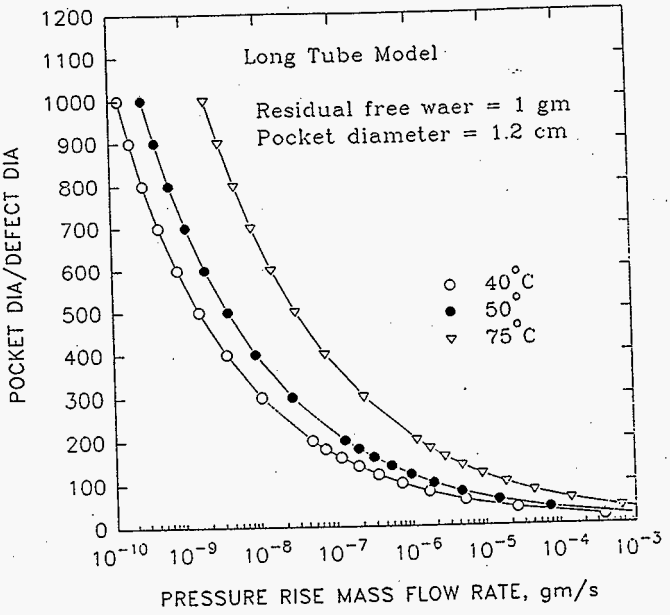

Figure 12. Ratio Pocket Diameter/Defect Diameter Versus Pressure Rise Mass Rate at Various Temperatures for Orifice Flow Model.

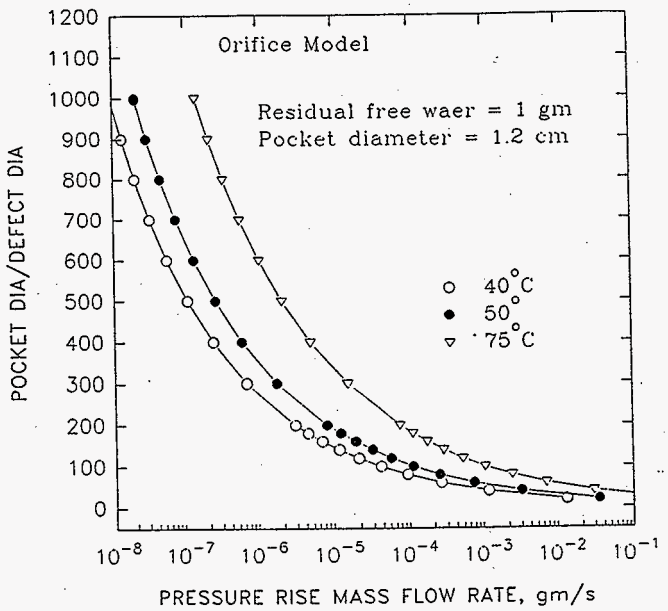

Figure 13. Pocket Diameter Versus Defect Radius at 50 °C and 75 °C for Various Amounts of Residual Free Water.

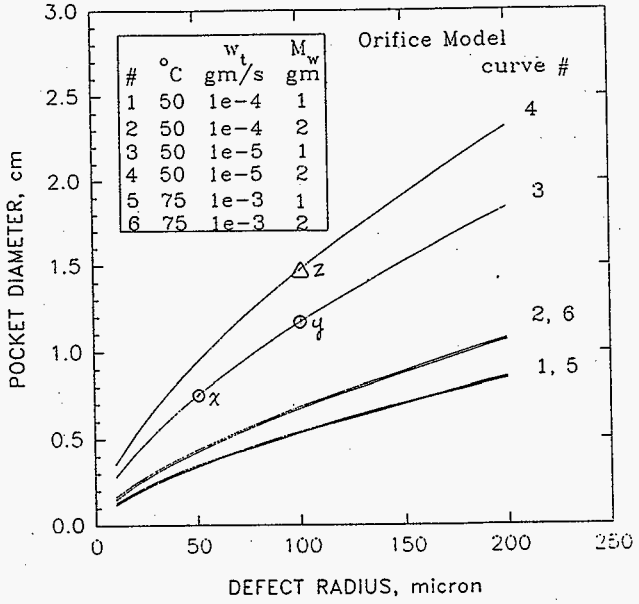

Figure 14. Defect Radius Determined from Pressure Rise Rate Ratio at 50 °C and 75 °C for Orifice Model.

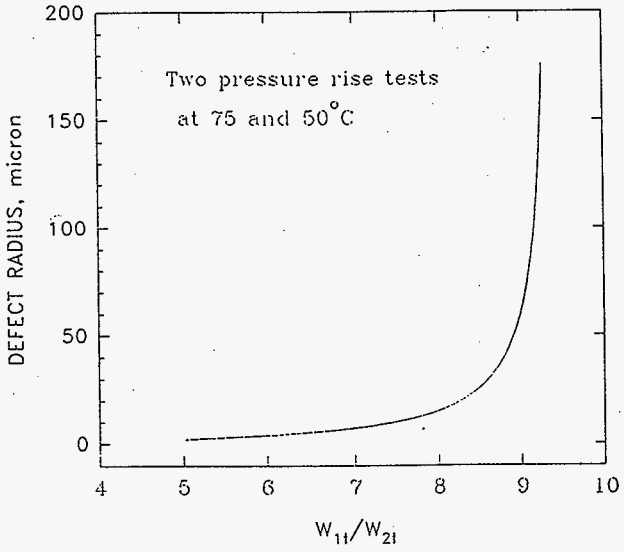

Figure 15. Drying of Spent Nuclear Fuel Element 0309M, Post-CVD Pressure Rise Test.

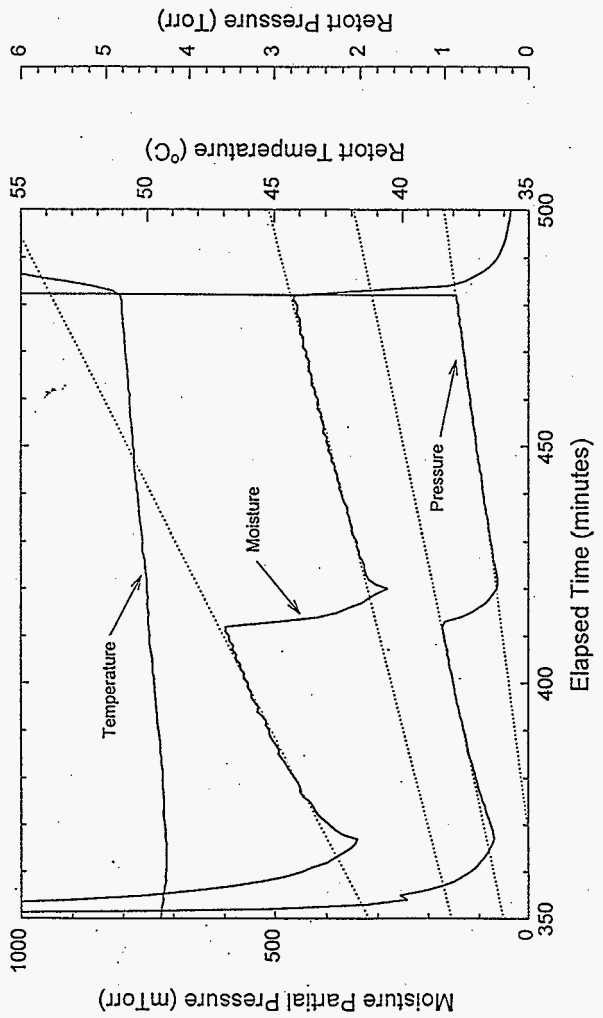

Figure 16. Drying of Spent Nuclear Fuel Element 5744U, Cold Vacuum Drying.

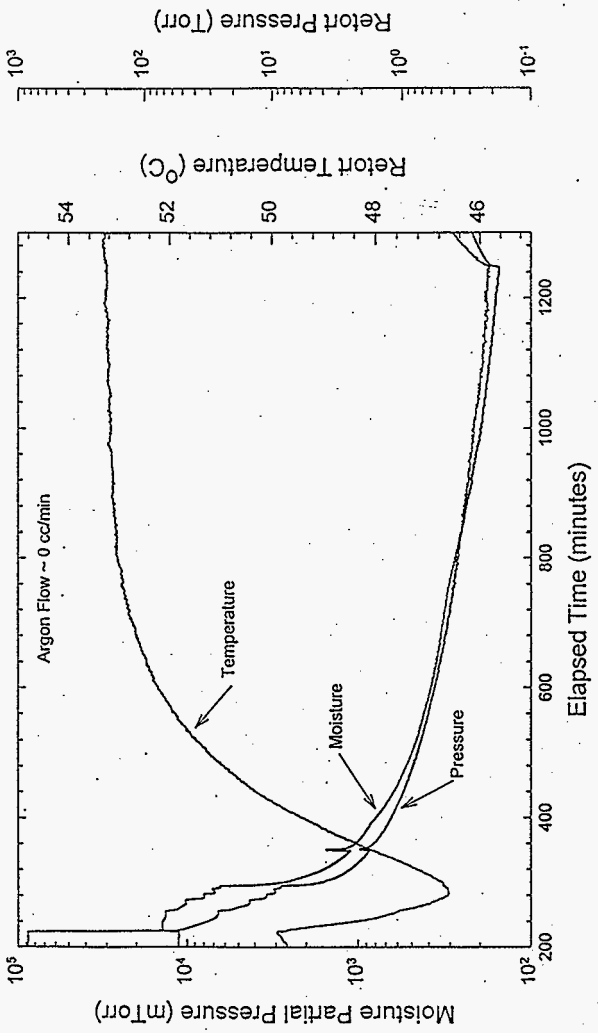

A P P E N D I X A

EVAPORATION RATE

This page intentionally left blank.

APPENDIX A

EVAPORATION RATE

According to the kinetic theory of gases the number of the vapor molecules striking unit area of a surface per unit time is (Bird 1976)

$$\nu = Nv_a/4 \tag{A1}$$

where N it the number of molecules per cm^3 and v_a is the mean velocity of the molecules. The mass of the vapor molecule striking the unit free surface per unit time is

$$G = \rho v_a/4 \tag{A2}$$

where ρ is the density of the vapor. For an ideal gas

$$\begin{aligned} PV &= nRT = GRT/M \\ \rho &= G/V = PM/RT \end{aligned} \tag{A3}$$

where M is the molecular mass in grams. Combining Equations (A2) and (A3) gives

$$G = PMv_a/4RT \tag{A4}$$

Gas dynamic theory also gives the pressure in terms of root-mean-square molecule speed, v_{rms}

$$P = \rho v_{rms}^2/3 \tag{A5}$$

The mean molecular velocity is related to the root-mean-square velocity through Maxwell-Boltzmann distribution of gas molecular velocity (Bird 1976) as follows.

$$\begin{aligned} v_a &= 2\sqrt{(2\kappa T/\pi m)} = 2\sqrt{(2RT/\pi N_A m)} \\ &= 2\sqrt{(2RT/\pi M)} \end{aligned} \tag{A6}$$

$$v_{rms} = \sqrt{(3\kappa T/m)} \tag{A7}$$

where $\kappa = 1.38054 \times 10^{-23}$ J/K is Boltzmann constant and m is mass of particle.

From Equations (A6) and (A7) the relationship between these two molecular velocities is

$$v_a = v_{rms}\sqrt{(8/3\pi)} \tag{A8}$$

Combining Equations (A4), (A5), and (A8) gives the rate of the vapor mass striking the surface

$$G = P\sqrt{(M/2\pi RT)} \tag{A9}$$

This page intentionally left blank.

A P P E N D I X B

SLIP FLOW RATE

This page intentionally left blank.

APPENDIX B

SLIP FLOW RATE

The viscous conductance corrected for slip is (Kennard 1938)

$$F=\frac{\pi a^4}{8\eta\ell}P_g\left(1+\frac{4\eta(2-f)}{faP_g}\left(\frac{\pi TR_o}{2M}\right)^{1/2}\right) \qquad (B1)$$

Equation (B1) can be rewritten to be

$$F=F_v+\frac{3\pi}{16}\frac{2-f}{f}F_t \qquad (B2)$$

$F_v = \pi a^4 P_g/8\eta\ell$

where F_v is the viscous conductance from Equation (9) and F_t the molecular flow conductance from Equation (10). The value of f in this equation is the transfer ratio of momentum ranging between 0.8 and 1.0. Equation (13) clearly combines the characteristics of both viscous and molecular ranges. An empirical relation with pressure dependence was formulated by Knudsen for slip flow in the transition range:

$$F = F_t(F_v/F_t + Z) \qquad (B3)$$

where

$Z = (1 + 2.507(a/L_a))/(1 + 3.095(a/L_a))$ and F_v/F_t can be expressed in terms of a/L_a using $\eta = 0.499\rho v_a L_a$ obtained from Equation (6), Equations (A3) and (A6).

$$F_v/F_t = 0.1472(a/L_a) \qquad (B4)$$

Equation (B3) also can be written in terms of viscous conductance F_v:

$$F = F_v\,(1 + 7.793(L_a/a)Z) \qquad (B5)$$

This page intentionally left blank.

A P P E N D I X C

INTERFACE IN FILLED PORE MODEL

This page intentionally left blank.

APPENDIX C

INTERFACE IN FILLED PORE MODEL

Assuming a 5-cm long pore with a radius of 50 μm is filled with water and the distance from the interface to the opening is y, an increment of y due to water vapor removal is

$$\Delta y = w\Delta t/\pi a^2\rho$$

Thus,

$$dy/dt = 2.1656 \times 10^{-6} F(P_2 - P_1)/\pi a^2 T \qquad (C1)$$

At the orifice $F = F_o$, use of Equation (C1) and Equation (12) gives

$$dy/dt = 0.3899/(1 + 0.375y/a)$$

$$y = ((25.44a^2 + 8.32at)^{1/2} - 5.333a)/2 \qquad (C2)$$

for

$$0 < y \leq 8a/3 \text{ and } T = 50\ ^\circ C$$

At $y = 8a/3$ [see Equation (12)], $t = 0.053$ s. As the interface recedes to $y = 8a/3$ (0.0133 cm), the flow rate is estimated for slip flow and $F = F_t(0.1472(a/L_a) + Z)$ as given in Equation (13). The change rate of y is computed using Equation (C1) and Equation (11).

$$dy/dt = 10.34a/y \qquad \text{for } y > 8a/3 \text{ and } T = 50\ ^\circ C$$

$$y^2/2 = 10.34at + C$$

$C = -0.00265$ for the initial conditions at $t = 0.053$ s for flow at orifice.

$$y = (20.68at - 0.0053)^{1/2}$$

$$t = (y^2 + 0.0053)/20.68a \qquad (C3)$$

DISTRIBUTION SHEET

To	From	Page 1 of 2
Distribution	SNF Characterization Project/ 2T720	Date April 1998
Project Title/Work Order		EDT No. 620804
RELEASE OF WATER TRAPPED IN DAMAGED FUEL SUBSURFACE VOIDS/ HNF-2191, Rev. 0		ECN No.

Name	MSIN	Text With All Attach.	Text Only	Attach./ Appendix Only	EDT/ECN Only
Fluor Daniel Hanford, Inc.					
E. W. Gerber	R3-11	X			
COGEMA Engineering Corporation					
A. L. Pajunen	R3-86	X			
Duke Engineering & Services Hanford, Inc.					
R. B. Baker	H0-40	X			
S. A. Chastain	H0-40	X			
D. R. Duncan	R3-86	X			
J. R. Frederickson	R3-86	X			
L. A. Lawrence (2)	H0-40	X			
B. J. Makenas	H0-40	X			
R. P. Omberg	H0-40	X			
J. A. Swenson	R3-11	X			
D. J. Trimble	H0-40	X			
SNF Project Files	R3-11	X			
Fluor Daniel Northwest					
L. J. Garvin	R3-26	X			
F. F. Huang	E6-15	X			
G. A. Ritter	H0-40	X			
R. E. Russell	E6-15	X			
D. A. Smith	R1-49	X			
J. B. Truitt	S0-04	X			
Lockheed Martin Services, Inc.					
Central Files	B1-07	X			

DISTRIBUTION SHEET

To	From	Page 2 of 2
Distribution	SNF Characterization Project/ 2T720	Date April 1998
Project Title/Work Order		EDT No. 620804
RELEASE OF WATER TRAPPED IN DAMAGED FUEL SUBSURFACE VOIDS/ HNF-2191, Rev. 0		ECN No.

Name	MSIN	Text With All Attach.	Text Only	Attach./ Appendix Only	EDT/ECN Only
Numatec Hanford Corporation					
G. P. Chevrier	R3-86	X			
E. R. Cramer	H0-34	X			
T. A. Flament	R3-86	X			
J. J. Irwin	R3-86	X			
C. R. Miska	R3-86	X			
J. P. Sloughter	H5-49	X			
Pacific Northwest National Laboratory					
J. Abrefah	P7-27	X			
S. C. Marschman	P7-27	X			
Technical Advisory Group					
J. C. DeVine	R3-11	X			
R. F. Williams	R3-11	X			
U.S. Department of Energy, Richland Operations Office					
R. M. Hiegel	S7-41	X			
P. G. Loscoe	S7-41	X			
E. D. Sellers	S7-41	X			
J. Shuen	S7-41	X			